Pulsed ion-beam induced nucleation and growth of Ge nanocrystals on SiO_2

N. P. Stepina,[a] A. V. Dvurechenskii, V. A. Armbrister, V. G. Kesler, P. L. Novikov, A. K. Gutakovskii, V. V. Kirienko, and Zh. V. Smagina
Institute of Semiconductor Physics, Siberian Branch of the Russian Academy of Sciences, prospekt Lavrent'eva 13, 630090 Novosibirsk, Russia

R. Groetzschel
Forschungszentrum Rossendorf, D–01328 Dresden, Germany

(Received 28 December 2006; accepted 26 February 2007; published online 30 March 2007)

Pulsed low-energy (200 eV) ion-beam induced nucleation during Ge deposition on thin SiO_2 film was used to form dense homogeneous arrays of Ge nanocrystals. The ion-beam action is shown to stimulate the nucleation of Ge nanocrystals when being applied after thin Ge layer deposition. Temperature and flux variation was used to optimize the nanocrystal size and array density required for memory device. Kinetic Monte Carlo simulation shows that ion impacts open an additional channel of atom displacement from a nanocrystal onto SiO_2 surface. This results both in a decrease in the average nanocrystal size and in an increase in nanocrystal density. © *2007 American Institute of Physics*. [DOI: 10.1063/1.2719163]

Nanocrystals (NCs) in a dielectric matrix have attracted much attention as a promising candidate for a charging nodes in a single-electron memory device (SEMD). An advantage of the nanofloating gate memory over the continuous floating gate is its improved endurance due to preventing lateral charge movement. Faster writing/erasing time, lower operating voltage, and longer retention time have been demonstrated in memory device based on Si NCs embedded in SiO_2.[1,2] Recently, King *et al.* showed that Ge-based SEMD has the superior properties over Si-based SEMD in terms of the writing/erasing time and the operating voltage.[3] Since then different methods were used for fabrication of Ge NCs in dielectric matrix, such as ion-beam synthesis,[4] oxidation and reduction of Ge/Si NCs,[5] rapid thermal annealing of cosputtered,[6] molecular beam epitaxy deposited,[7] and chemical-vapor deposited[3] layers, and pulsed-laser deposition.[8] However, space distribution of NCs within dielectric created by most of these techniques is random. To suppress the tunneling distance fluctuation, one should form in-plane distribution of NCs. Moreover, when using NCs for charge storage devices, the general requirements that can be placed upon the control are the size of NCs and their density and homogeneity in growth plane. That is the problem for most of the above-mentioned growth methods. Our preliminary results[9] pointed to the stimulation of Ge NC formation on relatively thick (~100 nm) SiO_2 films during pulsed low-energy (100–200 eV) ion-beam action. To understand the mechanism of pulsed ion-beam influence on the nucleation process and sputtering of SiO_2 layer, we study different regimes of Ge NC array growth on thin SiO_2 films typically used as tunnel layer in memory devices.

A 3.5 nm thick SiO_2 film was grown by thermal oxidation on (111) *p*-type silicon substrates (1 Ω cm) at 850 °C. After dioxide formation the wafers were washed, dried up, and inserted into the ultrahigh-vacuum (UHV) chamber of molecular beam epitaxy setup equipped with effusion cell for Ge. The system of ionization and acceleration of Ge^+ ions provided the degree of ionization of Ge molecular beam from 0.1% to 0.5%. Molecular beam deposition (MBD) was carried out at temperature varied from 250 to 400 °C. The total Ge effective thickness of deposition was 20 ML (monolayer). The rate of Ge deposition was varied between 0.08 and 0.19 ML/s. The generated ion-current pulses had duration of 0.5–1 s with ion energy of 200 eV. We compare two different regimes of ion-beam action. In the first case (called "capped SiO_2" regime) 3 Ge ML were deposited without ion-beam action. Pulsed ion-beam actions were applied in series at the effective Ge layer thicknesses of 3, 4, and 5 ML. In the second case (called "uncapped SiO_2" regime) ion implantation started simultaneously with Ge deposition and repeated after deposition of 1 and 2 ML. To prevent Ge oxidation some Ge samples were covered by thin (~5 nm) *a*-Si layer before taking them out from the UHV chamber.

The chemical content of the samples with open Ge NC surface was studied by electron spectroscopy for chemical analysis (ESCA) method after transferring the samples via ambient atmosphere to ESCA spectrometer. Figure 1 shows the detailed spectra of Ge 2*p* doublet and Si 2*p* for samples

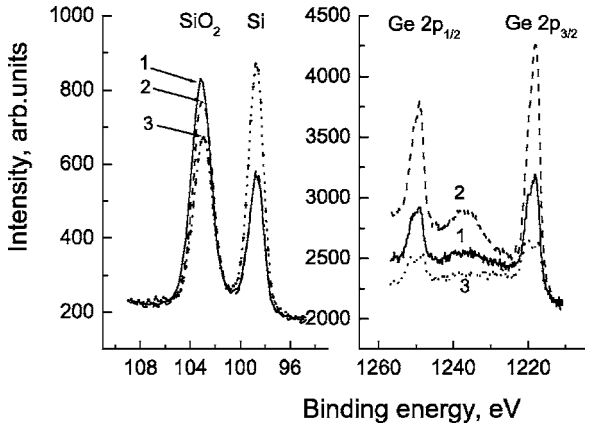

FIG. 1. ESCA spectra for Ge deposition at 300 °C with usual MBD (1) and ion-assisted MBD for "capped SiO_2" (2) and "uncapped SiO_2" (3) regimes. Left, peak of Si 2*p*; right, peak of Ge 2*p*.

[a]Electronic mail: stepina@isp.nsc.ru

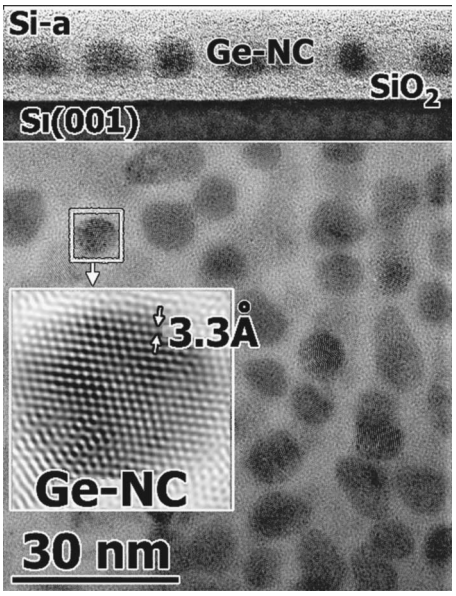

FIG. 2. HREM image (upper part, cross section; lower part, plan view) of nanocrystals on SiO_2 J_{Ge}=0.08 ML/s, T=250 °C.

grown by usual MBD (curve 1) as well as by ion-beam induced nucleation at capped SiO_2 (curve 2) and uncapped SiO_2 (curve 3) surface at T=300 °C. To find the influence of ion-beam action on tunnel oxide layer during Ge deposition, we analyzed the intensity of Si 2p line shown in the left part of Fig. 1. The thickness of tunnel oxide was evaluated from the intensity ratio of the oxide component Si 2p (103.0 eV) to the substrate component Si 2p (98.7 eV). The significant decrease in oxide thickness (from 4.2 to 2.4 nm) is observed in the case when ions irradiate an uncapped SiO_2 surface. Conventional and ion-assisted MBDs at capped SiO_2 surface keep dioxide layer thickness practically invariable. In all cases we did not reveal any changes in the stoichiometry of SiO_2 layer. The amount of Ge remaining at SiO_2 surface can be determined from the spectra of Ge 2p doublet shown in the right part of Fig. 1. Both Ge $2p_{1/2}$ and Ge $2p_{3/2}$ lines show pronounced superposition of two components with energy shift of 2.3 eV related to germanium in metallic and partially oxidized states, respectively. Precise analysis of Ge 2p and Ge 3d photoelectron lines characterized by significant difference in electron mean free path showed that GeO_x caps the pure germanium nuclei. The origin of GeO_x fraction is explained by the transferring of the samples to ESCA spectrometer via ambient atmosphere. Concentration of Ge deposited was determined from the integral intensity of Ge $2p_{3/2}$ peak. Both usual and ion-assisted MBDs at uncapped SiO_2 show smaller amount of Ge remaining on the SiO_2 surface than that for the capped SiO_2 regime, which gives 1.7 times higher Ge concentration. However, even in this case only ~30% of Ge remains on SiO_2 surface, indicating strong Ge desorption during the growth. Hereafter, we refer to capped SiO_2 regime when ion-assisted MBD is mentioned.

Figure 2 shows the structure of Ge NCs for high resolution electron microscopy (HREM) cross-section and plan-view images of samples, prepared using the chemical etching from the substrate side of the sample. Interplanar spacing corresponds to that for (111) planes in Ge.

Temperature and Ge flux were varied to optimize the parameters of NC ensemble. Homogeneous array of Ge ball-like NCs with ~6 nm average size was obtained by MBD

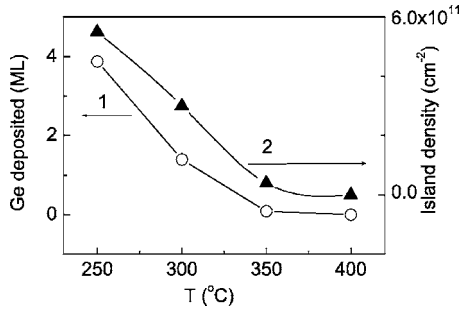

FIG. 3. NC density (HREM data, 2) and amount of Ge (RBS data, 1) dependence on growth temperature. J_{Ge}=0.125 ML/s.

using irradiation at 250 °C and Ge flux J_{Ge}=0.08 ML/s. Influence of growth temperature on NC density (HREM data) and Ge amount [Rutherford backscattering (RBS) data] is shown in Fig. 3. We have found that temperature affects only the density of this ensemble, keeping the island size practically unchanged. Ge desorption goes up as the substrate temperature increases. The detailed analysis of HREM data shows that ion-beam nucleation suppresses Ge desorption and decreases NC size and size dispersion (Fig. 4).

To clarify the mechanism of Ge NC formation and the role of ion irradiation, we have carried out the kinetic Monte Carlo (MC) simulation. The kinetics of NC formation was calculated using the "lattice gas" model,[10] which includes Ge atom deposition on SiO_2 surface, their surface diffusion, desorption, precipitation, and ion-beam action. The sites occupied by Ge atoms and SiO_2 were restricted to face-centered-cubic (fcc) lattice, which is well suited in describing precipitation in isotropic amorphous matrices (e.g., SiO_2). The lattice includes $128\times128\times32$ sites with cylindric boundary conditions in the lateral plane. The number and types of nearest neighbors to a Ge atom determine its interaction energy with other Ge atoms and SiO_2 matrix. The energy per one Ge–Ge bond in fcc lattice was taken to be equal to 0.2 eV, which corresponds to an activation surface diffusion energy of 0.8 eV at free Ge surface obtained from molecular dynamics calculation.[11] For Ge in SiO_2 environment the interaction energy per one neighbor site occupied by SiO_2 was chosen as much as 0.076 eV, which provides the reproduction of the experimental dependence of the amount of Ge remaining in the surface on the amount of Ge deposited. The kinetics of Ge atoms on the SiO_2 matrix surface is simulated by jumps to empty sites. The probability P of each jump is

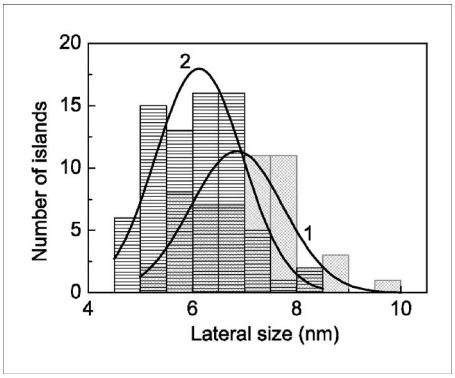

FIG. 4. NC size distribution for the irradiated (2) and nonirradiated (1) samples grown at T=250 °C and Ge flux J_{Ge}=0.1 ML/s.

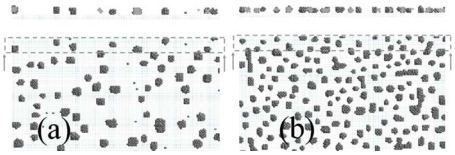

FIG. 5. Ge NCs on SiO_2 simulated by MC without (a) and with (b) ion-beam action. The upper image is a cross section of the same array within the region marked with a dashed rectangle on the plan view. $T=350\,^{\circ}\mathrm{C}$, $J_{\mathrm{Ge}}=0.1$ ML/s.

$$P \propto e^{(n_i-n_f)E/kT}, \tag{1}$$

where n_i and n_f are the numbers of neighbors of the jumping atom in the initial and final positions, respectively, E is a bond energy per one neighbor, k is the Boltzmann constant, T and is the temperature. Figure 5(a) presents the results of MC simulation of Ge NCs (plan-view and cross-section images) formed on SiO_2 without ion-beam action. The NCs have isotropic shape, corresponding to minimal surface energy, as would be expected for thermal equilibrium condition at nonwettable SiO_2 surface. The growth is a kinetic rather than an equilibrium process. However, our calculations showed that the surface energy minimization remains a dominating factor of NC formation. In the frame of this model an irradiation effect was described by the concept of collisional mixing, i.e., the displacements of atoms. In the simulation process each Ge atom has a probability P_{DP} to be displaced by a distance R during one MC step:

$$P_{\mathrm{DP}} = qe^{-R/\lambda}, \tag{2}$$

where λ is the length of displacement, depending on an ion energy, and q is the factor proportional to the ion flux density. We neglected the known effects of temperature-dependent ion-solid interactions, which are observed at temperatures above 300 °C and ion energies of about 100 eV and lower.[12] Ion-beam action results in the smaller NC size and the higher NC density [Fig. 5(b)] due to precipitation and nucleation of new NCs by atoms knocked out from initial NCs to the SiO_2 surface.

In conclusion we have shown that pulsed low-energy ion-beam nucleation during Ge deposition on SiO_2 films allows the suppression of Ge desorption, increases the density of Ge nanocrystals, and decreases the average nanocrystal size and size dispersion.

This work was supported by the Russian Foundation for Basic Research (Grant No. 06-02-08077).

[1] S. Tiwari, F. Rana, H. Hanati, A. Hartstein, E. F. Crabble, and K. Chan, Appl. Phys. Lett. **68**, 13770 (1996).
[2] D. W. Kim, T. Kim, and S. K. Benerjee, IEEE Trans. Electron Devices **50**, 1823 (2003).
[3] Y. C. King, T. J. King, and C. Hu, IEEE Trans. Electron Devices **48**, 696 (2001).
[4] P. Normand, E. Kapetanakis, D. Tsoukalas, G. Kamoulakos, K. Beltsios, J. Van Den Berg, and S. Zhang, Mater. Sci. Eng., C **15**, 145 (2001).
[5] T. Sass, V. Zela, A. Gustafsson, I. Pietzonka, and W. Seifert, Appl. Phys. Lett. **81**, 3455 (2002).
[6] W. K. Choi, W. K. Chim, C. L. Heng, L. W. Teo, Vincent Ho, V. Ng, D. A. Antoniadis, and E. A. Fitzgerald, Appl. Phys. Lett. **81**, 2014 (2002).
[7] A. Kanjilal, J. L. Hansen, P. Gaiduk, A. N. Larsen, N. Cherkashin, A. Claverie, P. Normand, E. Kapelanakis, D. Skarlatos, and D. Tsoukalas, Appl. Phys. Lett. **82**, 1212 (2003).
[8] X. B. Lu, P. F. Lee, and J. Y. Dai, Appl. Phys. Lett. **86**, 203111 (2005).
[9] A. V. Dvurechenskii, P. L. Novikov, Y. Khang, Zh. V. Smagina, V. A. Armbrister, and A. K. Gutakovskii, Proc. SPIE **6260**, 626006 (2006).
[10] P. Novikov, K.-H. Heinig, A. Larsen, and A. Dvurechenskii, Nucl. Instrum. Methods Phys. Res. B **191**, 462 (2002).
[11] D. Srivastava and B. J. Garrison, Phys. Rev. B **46**, 1472 (1994).
[12] Z. Wang and E. G. Seebauer, Phys. Rev. Lett. **95**, 015501 (2005).